CHAPTER IV

RESULTS AND DISCUSSION

4.1 Preparation of a bared monolithic silica column

The monolithic silica capillary column was prepared from a mixture of tetramethoxysilane (TMOS) and methyltrimethoxysilane (MTMS) (ratio 3:1) as followed by Ye et al [10] in 200 μm I.D. of capillary column via sol-gel process. There were many factors which cause the poor efficiency of column. The small bubbles in the mixture solution introducing into the capillary column were one of the problems that occurred in the step of mixture introduction. This problem affected the homogeneity of silica monolithic skeleton which made the poor plate height (more than 20 μm). The morphology of silica skeleton is shown in Figure 4.1 (a). The poor attachment of silica monoliths to the inner wall of capillary column and the irregular pore structure were observed. Therefore, the bared monolithic silica columns that used in this work were given from Dr.Wasura who was studied a Ph.D. at Department of Chemistry, Faculty of Science, Chulalongkorn University and done a short research at Tanaka's laboratory. Wasura synthesized high efficiency columns at Tanaka's laboratory and the morphology of the columns was shown in Figure 4.1 (b).

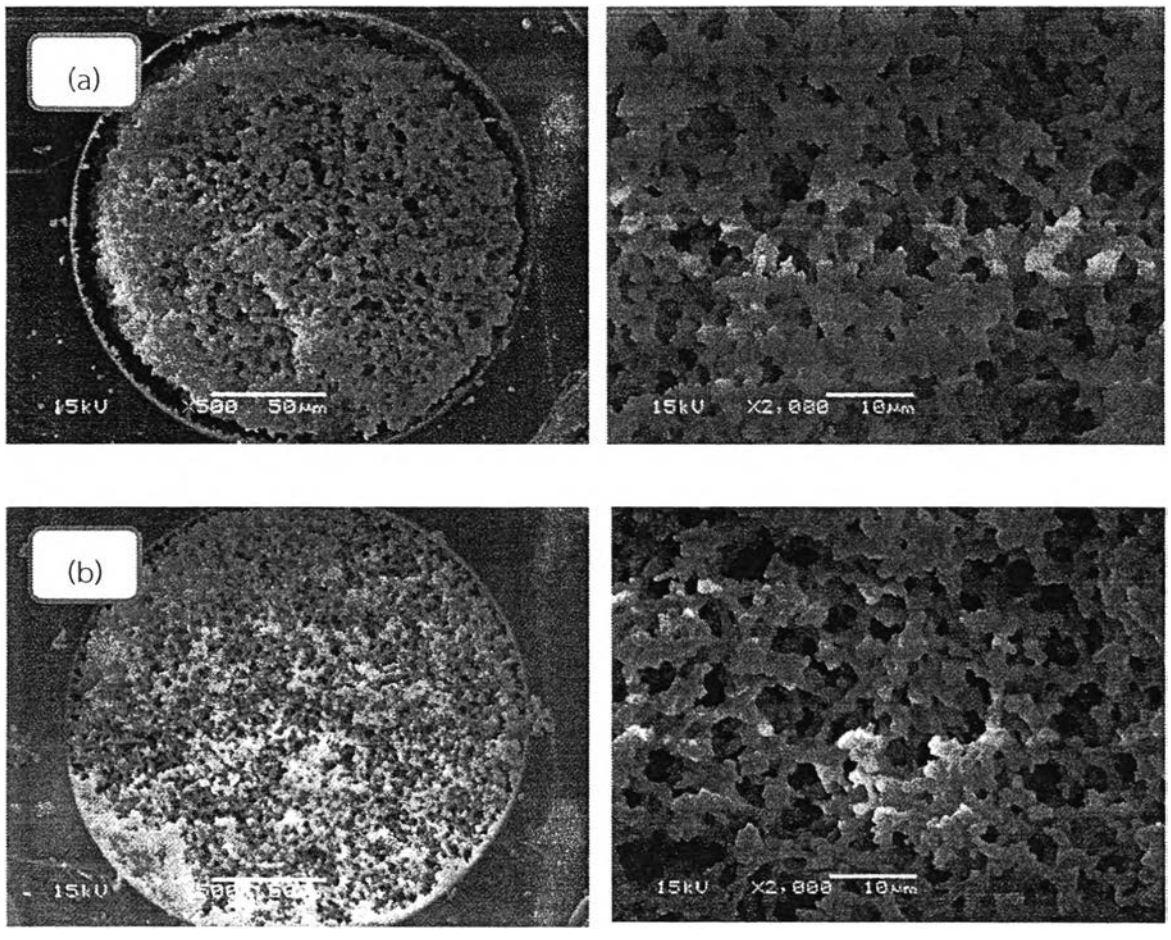

Figure 4.1 SEM images of the cross section of a bared silica monolithic capillary column (a) preparing in Thailand (b) column given by Dr.Wasura.

Stationary phase containing C_{18}-AP or C_{14}-amine embedded groups were functionalized by different methods. The proposed structures of the columns were shown in Figure 4.2 The high porosity, in other word, the high permeability is the advantage of monolithic columns which provides fast separation at high linear velocities. The porosity of the silica monolithic column was reported 2-30 times higher than that of particle packed column with 5-µm particles [43].

The permeability (K) was calculated by using Eq. 4.1 (η, viscosity of the mobile phase; L, column length; ΔP, back pressure; u, linear velocity of mobile phase and ε_T, total column porosity) [44] in a 80% methanol.

$$K = \frac{u\eta L\varepsilon_T}{\Delta P} \tag{4.1}$$

In this study, 80% methanol was used as a mobile phase which the viscosity of mobile phase was 1.12 × 10-3 Pa.s [45]. The total porosity of silica monolithic column usually exceeds 90% of the column volume [46]. The permeability of both columns after modification are shown in Table 4.1.

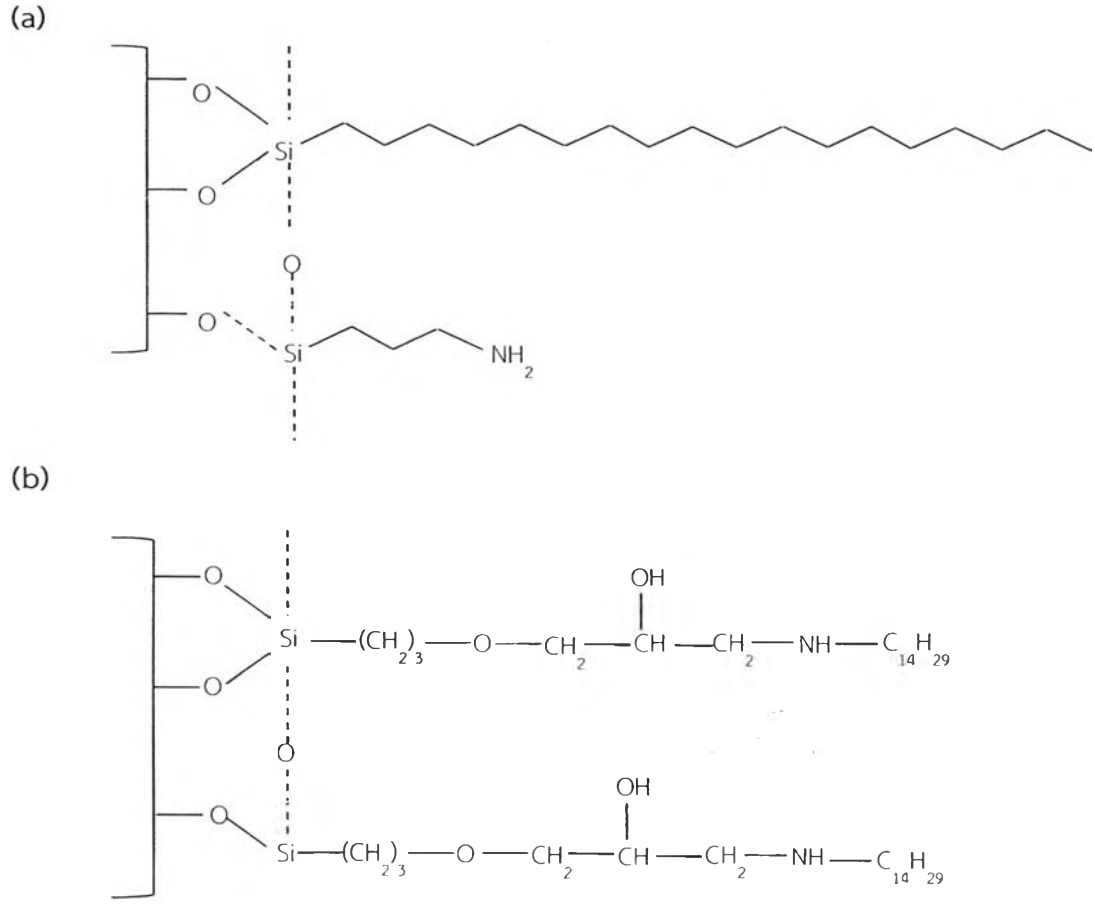

Figure 4.2 The proposed structure of columns (a) C_{18}-AP column (b) C_{14}-amine embedded column [30].

Table 4.1 The permeability of the one-step (C_{18}-AP) and two-step (C_{14}-amine embedded) modification columns.

Column	u (mm/s)	η (Pa.s)	ε_T	L (mm)	ΔP (Pa)	K (m^2)
C_{18}-AP	1.0	1.12×10^{-3}	0.90	443	4.52×10^{6}	7.65×10^{-14}
C_{14}-amine embedded				360	4.91×10^{6}	7.36×10^{-14}

As Table 4.1, the permeability of both columns was comparable. Using the correlation between pore size, skeleton size, HETP and permeability of silica monolithic column in Table 4.2, the prepared columns predicted to have a skeleton size of 1.0 μm, a macropore size of 2.0 μm and HETP of 7.9 μm. The permeability of the prepared columns were similar to the packed column with particle size of 8.9-9.2 μm but the efficiency was as good as the packed column with the particle size of 5-μm [47].

Table 4.2 Correlation between average pore size, skeleton size, HETP and permeability of silica monolithic column [47].

Permeability (10^{-14} m^2)	Skeleton size (μm)	Macropore size (μm)	HETP (μm)
8	1.0	2.0	7.9
15	1.1	2.2	8.7
19	1.5	2.0	9.3
25	1.4	2.8	10.5
56	2.0	4.5	11.9
130	2.0	8.0	12.5

4.2 Chromatographic characterizations by Tanaka's Test

4.2.1 Overview of chromatographic performance

The prepared columns, C_{18}-AP column and C_{14}-amine embedded, contained alkyl chains and polar groups as shown in Figure 4.2. The reversed-phase mechanism was expected to be a main mechanism for separation of analytes on both columns. The weak anion exchange mechanism was involved in some separation. We expected that the different phase structure of the columns should be exhibited in the chromatographic differences. As the proposed structure, we expected that the tetradecyl group on the two-step modification method's column (C_{14}-amine embedded column) might displayed the lower hydrophobicity than the one-step modification method's column (C_{18}-AP column) which has octadecyl group. In addition, the ion exchange mechanism and the shape selectivity of both columns should not significantly different since both columns contained a similar polar group (amine group).

Tanaka's test was chosen to primarily evaluated column performances. The results of the prepared mixed-mode columns (C_{18}-AP column and C_{14}-amine embedded column) were shown in Table 4.3 and compared to the reversed-phase column (C_{18} column) reported by Napug [1]. The discussion of each property was described in detail in the next section.

Table 4.3 Chromatographic characterization comparison by Tanaka [2].

Properties of Stationary Phase	Probes	C_{18}-AP column		C_{14}-amine embedded column		C_{18} column[a]		Mobile Phase
		k′	α	k′	α	k′	α	
Hydrophobicity	Pentylbenzene	0.684	1.43	0.369	1.54	0.458	1.35	80% CH_3OH
	Butylbenzene	0.477		0.238		0.339		
Shape Selectivity	Triphenylene	0.632	1.57	0.771	1.18	0.633	1.41	80% CH_3OH
	o-terphenyl	0.402		0.649		0.450		
Ion Exchange activity at pH 2.7	Benzylamine	(-0.101)	(-0.17)	0.108	0.39	0.045	0.16	30% CH_3OH, pH 2.7
	Phenol	0.608		0.280		0.286		
Ion Exchange activity at pH 7.6	Benzylamine	0.190	0.29	0.394	1.57	0.550	2.07	30% CH_3OH, pH 7.6
	Phenol	0.654		0.250		0.266		
Silanophilic Interaction	Caffeine	0.377	0.56	0.209	0.69	0.292	1.11	30% CH_3OH
	Phenol	0.667		0.301		0.263		

[a]: The Tanaka's test of C_{18} column were taken from Napug [1].

4.2.2 Hydrophobicity

The hydrophobicity was considered from the ratio of retention factors (α_{CH2}) of pentylbenzene (k'_P) and butylbenzene (k'_B) as shown in Table 4.3. Although the selectivity of hydrophobic probe on C_{14}-amine embedded column (α_{CH2} = 1.54) was higher than that on C_{18}-AP column (α_{CH2} = 1.43), the retention factors of hydrophobic probes (k'_P and k'_B) on C_{14}-amine embedded column (k'_P = 0.369 and k'_B = 0.238) were lower than those on C_{18}-AP column (k'_P = 0.684 and k'_B = 0.477). This implied that the analytes were retained in C_{14}-amine embedded column less than C_{18}-AP column and indicated that C_{14}-amine embedded column displayed lower hydrophobicity. This might occur from two reasons: (i) the polar groups (-OH and -NH) as shown in Figure 4.2 (b) reduced the hydrophobicity of column or (ii) there was few percentage of the alkyl group (tetradecyl) on C_{14}-amine embedded column. However, the low hydrophobicity of C_{14}-amine embedded column still had a good selectivity for the test probes as well as C_{18}-AP column based on reversed phase mechanism. Moreover, the hydrophobicity of the prepared mixed-mode column were slightly better than that of the reversed-phase column (C_{18} column).

4.2.3 Shape Selectivity

The ratio of retention factor of triphenylene (planar) and o-terphenyl (nonplanar) ($\alpha_{TR/O}$) was calculated. This value was used to define the ability of a phase to distinguish between two compounds which differ in their shape (planar and nonplanar structure). As shown in Table 4.3, the selectivity of C_{18}-AP column ($\alpha_{TR/O}$ = 1.57) was better than that of C_{14}-amine embedded column ($\alpha_{TR/O}$ = 1.18). However, the retention factors of triphenylene and o-terphenyl on C_{14}-amine embedded column (k'_{TR} = 0.771 and k'_O= 0.649) were higher than those on C_{18}-AP column (k'_{TR} = 0.633 and k'_O= 0.402). The different retention factors on the phases can be explained by slot model. It implied that triphenylene can slot in between the alkyl chains whereas *o*-terphenyl is less likely. The higher retentivity of C_{14}-amine embedded column might be explained by the slot size increase, so the analytes can

penetrated through the slot and had an affinity with phase better than C_{18}-AP column.

4.2.4 Ion exchange and silanol activity

Benzylamine and phenol were used to be the test probes for ion exchange at pH 2.7 and 7.6. At pH 2.7, the residual silanols were protonated and the polar groups were partially protonated. The reversed phase mechanism might be the major mechanism. As the reversed phase mechanism, benzylamine, which has lower hydrophobicity than phenol (log P_{ow} of benzylamine = 1.09 [48], logP_{ow} of phenol = 1.47 [49]), was less retained in both columns (k'_B= -0.101 for C_{18}-AP column and k'_B= 0.108 for C_{14}-amine embedded column). As the results, benzylamine on C_{18}-AP column was retained less than void volumn marker (thiourea) because it might be the effect of the electrostatic repulsion between positively charge of benzylamine and polar groups. However, benzylamine was retained longer than thiourea on C_{14}-amine embedded column. It can be explained that benzylamine was driven with positively charge of polar group but there was a small percentage of polar group which arise from unreacted spacer.

At pH 7.6, the total ion exchange activity which are the deprotonated silanol groups and protonated polar groups, were determined. For C_{18}-AP column, benzylamine came out before phenol based on reversed phase mechanism (k'_B= 0.190 and k'_P= 0.654). In contrast, the elution order of benzylamine and phenol was reversed on C_{14}-amine embedded column (k'_B= 0.394 and k'_P= 0.250). The unreacted spacer was suspected to decompose from epoxy form into hydroxyl form as seen in Figure 4.3. At this condition, the hydroxyl groups were deprotonated and can react with the positively charge of benzylamine.

As the results, the polar groups can shield the silanol group but C_{14}-amine embedded column (two-step modification column) still had the unreacted problem. For silanol activity, there was no significant difference in silanol activity ($\alpha_{C/P}$= 0.56 for C_{18}-AP column and $\alpha_{C/P}$= 0.77 for C_{14}-amine embedded column) between the both columns. There were two reasons that can be explained: (i) the

both columns have a few residual silanol or (ii) the polar groups on the both columns reduced the accessibility of silanol groups to test probes. However, the retention factors of test probe (caffeine and phenol) on C_{14}-amine embedded column were higher than that on C_{18}-AP column. It can be explained that the unreacted spacer can decompose to a hydroxyl form. That form might interact with the test probes.

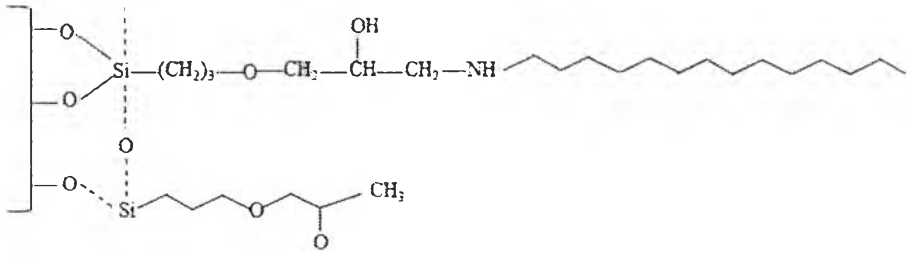

Figure 4.3 The proposed structure of unreacted C_{14}-amine embedded groups

4.3 Column performance of C_{18}-AP and C_{14}-amine embedded monolithic silica columns

4.3.1 Separation of alkylbenzene

As results from Tanaka's test, a reversed phase mechanism was the major mechanism with long alkyl chains of both columns. Four alkylbenzene (ethylbenzene, propylbenzene, butylbenzene and pentylbenzene) at concentration of 50 mgL^{-1} were used to compare the separation performance of two columns which differ with modification method (one-step and two-step modification method) and using 80% methanol as a mobile phase.

Table 4.4 The retention factors of alkylbenzene on the C_{18}-AP and C_{14}-amine embedded columns.

Peaks No.	Analytes	Retention factor (k´)	
		C_{18}-AP column	C_{14}-amine embedded columns
2	Ethylbenzene	0.239	0.067
3	Propylbenzene	0.334	0.119
4	Butylbenzene	0.478	0.216
5	Pentylbenzene	0.684	0.407

As Table 4.4, the retention factors of alkylbenzenes on C_{14}-amine embedded column were lower than that on C_{18}-AP column. The elution order on both columns were similar and based on reversed phase mechanism. It indicated that C_{14}-amine embedded column displayed lower hydrophobicity than C_{18}-AP column. There were two reasons of low hydrophobicity on C_{14}-amine embedded column which arised from (i) the polar groups on the phase and (ii) low percentage of long akyl chains (the unreacted phase as seen in Figure 4.3).

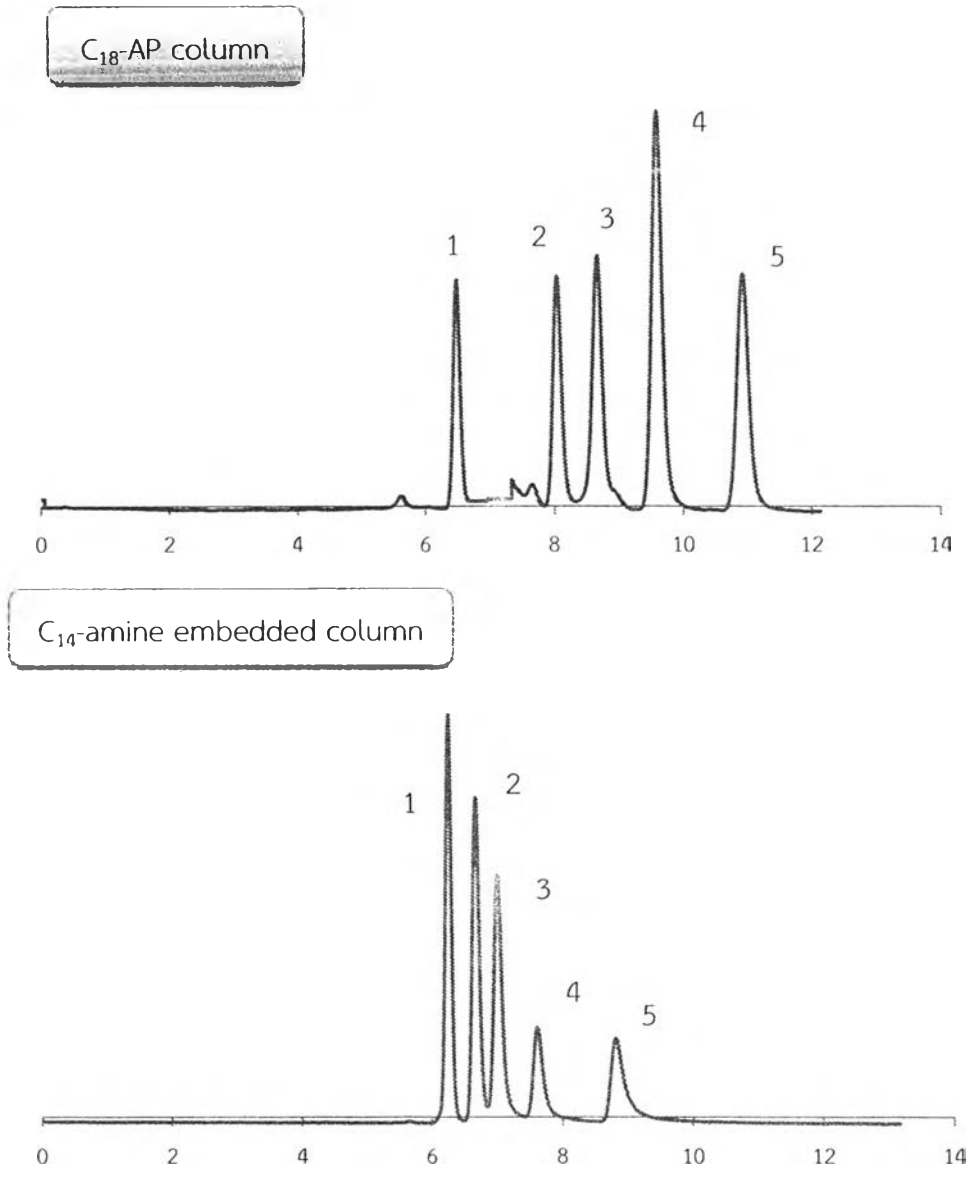

Figure 4.4 Chromatogram for the separation of alkylbenzene using a C_{18}-AP column and a C_{14}-amine embedded column. Mobile phase: 80% methanol, linear velocity: u = 1.0 mm/s, detection wavelength = 210 nm; Compounds (1) thiourea (2) ethylbenzene (3) propylbenzene (4) butylbenzene and (5) pentylbenzene

4.3.2 Separation of benzoic acids

The mixture of polar acids, which are composed of 4-hydroxybenzoic acid, 3,4-dihydroxybenzoic acid and 3,4,5-trihydroxybenzoic acid, were used to compare the difference amongst the two types of stationary phase by using 25:75 methanol/ 0.02 M phosphate buffer. At this condition, silanol groups and polar acids were suppressed with acidic mobile phase. The elution order was thiourea < 3,4,5-trihydroxybenzoic acid < 3,4-dihydroxybenzoic acid < 4-hydroxybenzoic acid. Two interactions between analytes and phase (the hydrophobic interaction between analytes and alkyl chain, including hydrogen bonding between carboxyl/hydroxyl groups and the residual silanol groups) were predicted. Thus, the column that showed a high hydrophobicity and high silanol activity should display the high retention. However, the retention factors of these polar acids on C_{14}-amine embedded column were higher than that on C_{18}-AP column, especially 4-hydroxybenzoic acid.

Table 4.5 pK_a, Log octanol/water coefficients (Log P_{ow}) and the retention factor of polar acids.

Analytes	pK_{a1}	pK_{a2}	pK_{a3}	pK_{a4}	Log P_{ow}	Retention factor (k')	
						C_{18}-AP column	C_{14}-amine embedded column
4-hydroxybenzoic acid	4.58	9.23	-	-	1.37	0.3958	1.0534
3,4-dihydroxybenzoic acid	4.50	8.70	12.80	-	1.15	0.1726	0.1896
3,4,5-trihydroxybenzoic acid	4.48	4.47	4.47	4..41	0.70	0.0788	0.0826

As described above, the second reaction of C_{14}-amine embedded column (two-step modification column) may not be 100% completed. Besides two interactions that were predicted, the third interaction may occur on C_{14}-amine embedded column from the unreacted epoxy groups. The unreacted epoxy groups may lead to the hydrogen bonding with analytes which affected the retentivity of compounds especially 4-hydroxybenzoic acid which might occurred from the less steric effect than the other compounds.

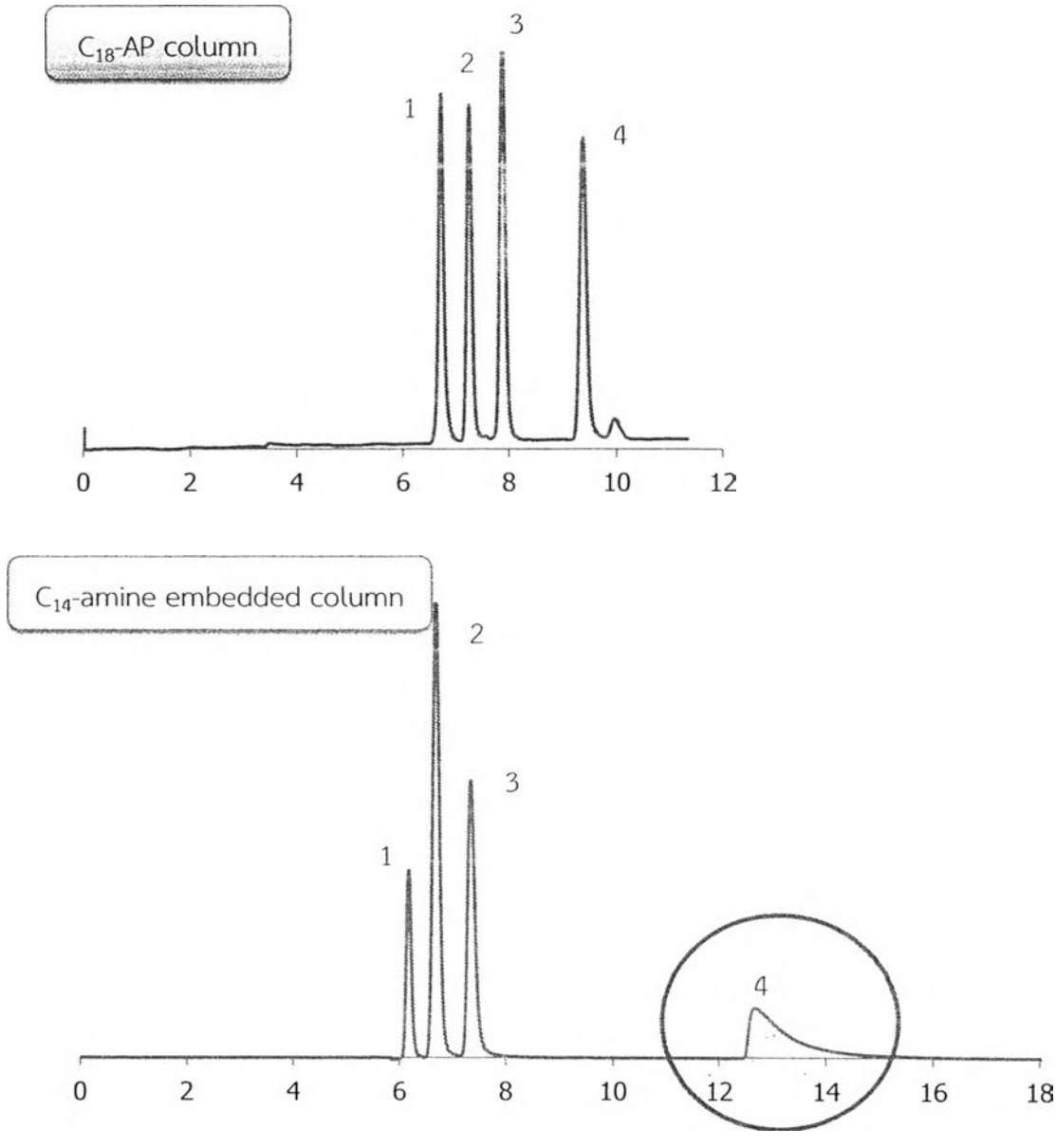

Figure 4.5 Chromatogram for the separation of benzoic acids using a C_{18}-AP column and a C_{14}-amine embedded column. Mobile phase: methanol: 0.02 M phosphate buffer pH 2.5 (25:75), linear velocity: u = 1.0 mm/s, detection wavelength = 210 nm; Compounds: (1) thiourea (2) 3,4,5-trihydroxybenzoic acid (3) 3,4-dihydroxybenzoic acid and (4) 4-hydroxybenzoic acid.

4.3.3 Separation of halobenzoate anions

Halobenzoate anions were performed using a mobile phase of 60% methanol in 0.02 M phosphate buffer pH 6.7. These analytes were ionized form at this condition according to their pK_a value (as seen in Table 4.6) and amino groups on both columns were partially protonated. The major mechanism of benzoate anions separation was ion-exchange mechanism. The electron withdrawing groups increase the acidic strength of the benzoate anions which is the increasing of ion strength. As the electron withdrawing group on each benzoic acid (-F, -Cl and –di Cl), the ion strength of benzoate anions increased with increase in the number of halogen atoms (the electron withdrawing group). As the results, the elution order was 3-fluorobenzoic acid < 3-chlorobenzoic acid < 3,4-dichlorobenzoic acid. Ion strength of 3,4-dichlorobenzoate anion was highest and occurred the best anion exchange which result to the highest retention. As the same number of halogen, 3-fluorobenzoic acid was retained less than 3-chlorobenzoic acid because fluoride at meta withdrawed the electron density less than chloride atom. As that reason, ion strength of 3-fluorobenzoate anion was less than 3-chlorobenzoate anion. The retention factors of solutes on C_{14}-amine embedded column were less than those on C_{18}-AP column. It can be explained that solutes were less retained on C_{14}-amine embedded column because of a small percentage of amino embedded. However all sample could not be separate on the C_{18} column [1].

Table 4.6 The retention factors of benzoate anions

Analytes	Retention factor (k')	
	C_{18}-AP column	C_{14}-amine embedded column
3-Fluorobenzoic acid	0.095	0.047
3-Chlorobenzoic acid	0.179	0.092
3,4-dichlorobenzoic acid	0.373	0.189

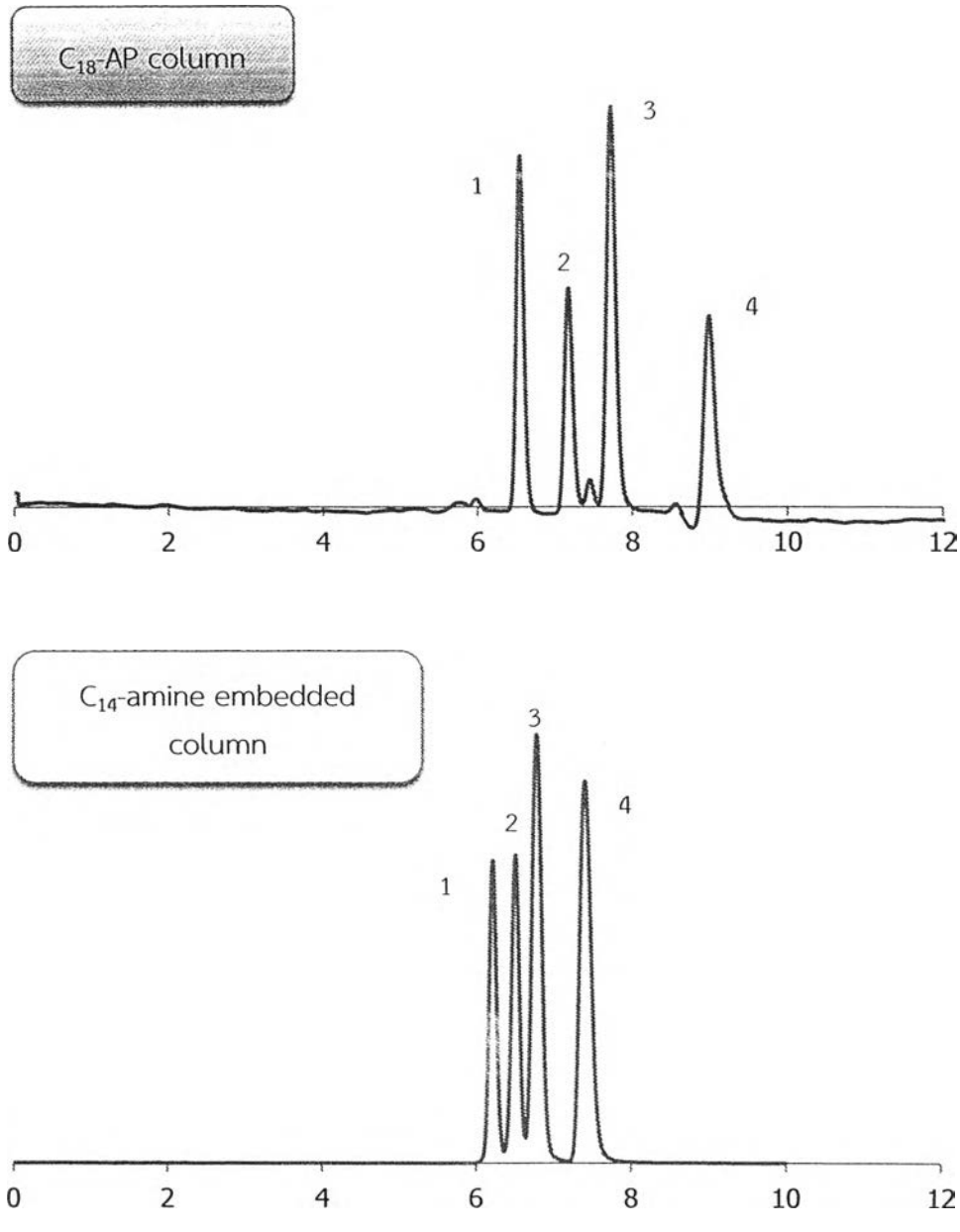

Figure 4.6 Chromatogram for the separation of benzoate anions using a C_{18}-AP column and a C_{14}-amine embedded column. Mobile phase: methanol: 0.02 M phosphate buffer pH 6.7 (60:40), linear velocity: u = 1.0 mm/s, detection wavelength = 210 nm; Compounds: (1) thiourea (2) 3-fluorobenzoic acid (3) 3-chlorobenzoic acid (4) 3,4-dichlorobenzoic acid

4.3.4 Separation of basic compounds

The separation of basic compounds is the challenge for analyst with tailing peak problem. The tailing peak problem occurred from the interaction between the deprotonated silanol and protonated basic compounds. The reversed stationary phases with polar groups were developed to overcome this problem. Thus we predicted that the polar groups on C_{18}-AP column and C_{14}-amine embedded column would reduce the tailing peak. At this condition, the residual silanols were deprotonated and the polar groups were protonated. The elution order was aniline < N-methylaniline < benzylamine < diphenylamine with hydrophobic mechanism. The retention factors of basic compounds on C_{14}-amine embedded column were less than those on C_{18}-AP column, which related to a low hydrophobicity of C_{14}-amine embedded column. As peak asymmetry in Table 4.7, the peak tailing of basic compounds were observed on C_{14}-amine embedded column which might occur from (i) the residual silanol groups or (ii) the decomposed of unreacted spacer (hydroxyl groups).

Table 4.7 The retention factors and peak symmetry comparison.

Peaks	Solutes	C_{18}-AP column		C_{14}-amine embedded column	
		Retention factor (k')	Asymmetry	Retention factor (k')	Asymmetry
2	aniline	0.093	1.06	0.082	1.08
3	N-methylaniline	0.168	1.21	0.124	1.31
4	benzylamine	0.289	1.38	0.224	1.42
5	diphenylamine	0.394	1.49	0.319	1.90

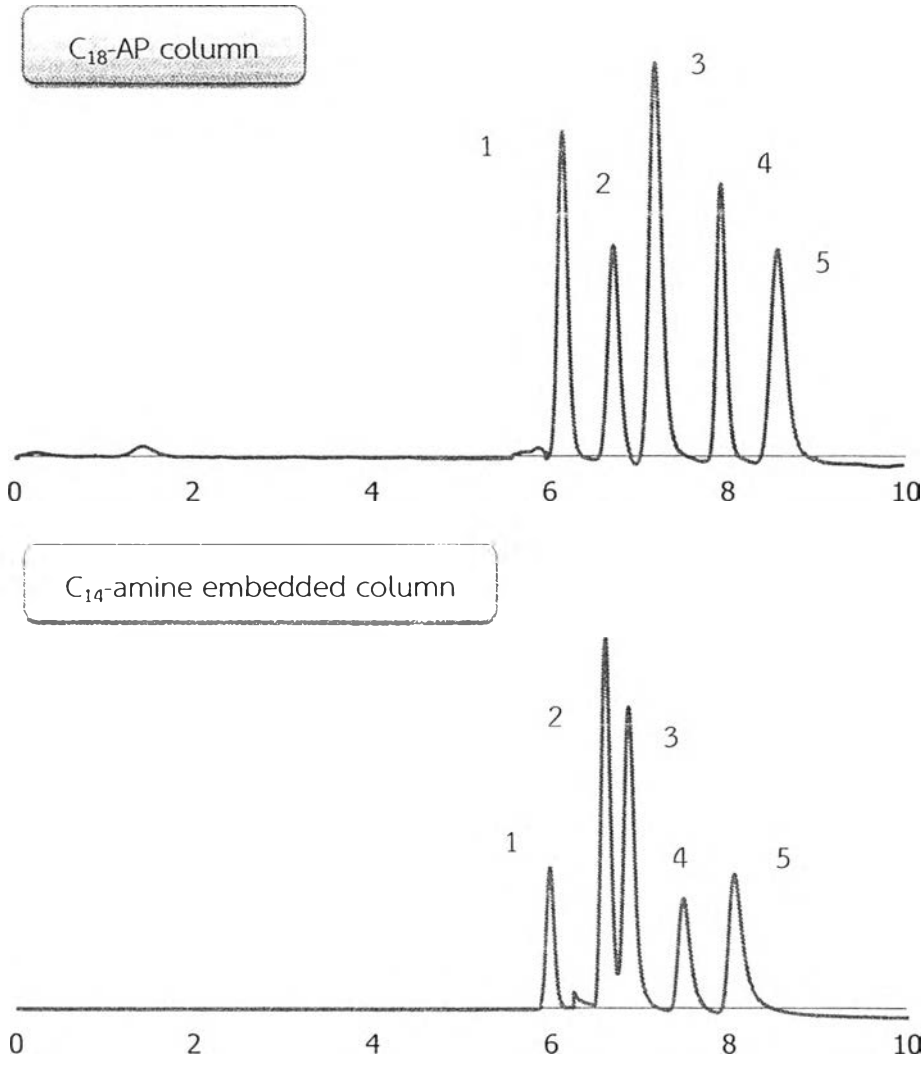

Figure 4.7 Chromatogram for the separation of basic compounds using a C_{18}-AP column and a C_{14}-amine embedded column. Mobile phase: methanol: 0.01 M phosphate buffer pH 7.5 (55:45), linear velocity: u = 1.0 mm/s, detection wavelength = 210 nm; Compounds: (1) thiourea (2) aniline (3) N-methylaniline (4) benzylamine and (5) diphenylamine

4.3.5 Separation of polycyclic aromatic hydrocarbons (PAHs)

In order to assess shape selectivity, PAHs, which composed of anthracene, fluoranthene, triphenylene and benzo(k)fluoranthene, were used. The test probes were separated by using 70% methanol as a mobile phase. As results, triphenylene and benzo(k)fluoranthene were retained on C_{14}-amine embedded column longer than on C_{18}-AP column. It can be explained with "slot model". It means C_{14}-amine embedded column has a bigger slot than C_{18}-AP column as proposed in Figure 4.8. Therefore the solutes that can penetrate through the slot retained more on the column. However anthracene and fluoranthene were less retained on C_{14}-amine embedded column than on C_{18}-AP column. Because of the small molecules of anthracene and fluoranthene, the test probes can penetrate through the slot of both columns. As described in section 4.3.1, C_{14}-amine embedded column showed lower hydrophobicity than C_{18}-AP column, so the test probes were less retained on C_{14}-amine embedded column.

Table 4.8 The retention of PAHs comparison.

Peaks	Solutes	Retention factor (k')	
		C_{18}-AP column	C_{14}-amine embedded column
2	anthracene	0.500	0.421
3	fluoranthene	0.583	0.532
4	triphenylene	0.695	0.786
5	benzo(k)fluoranthene	0.798	0.948

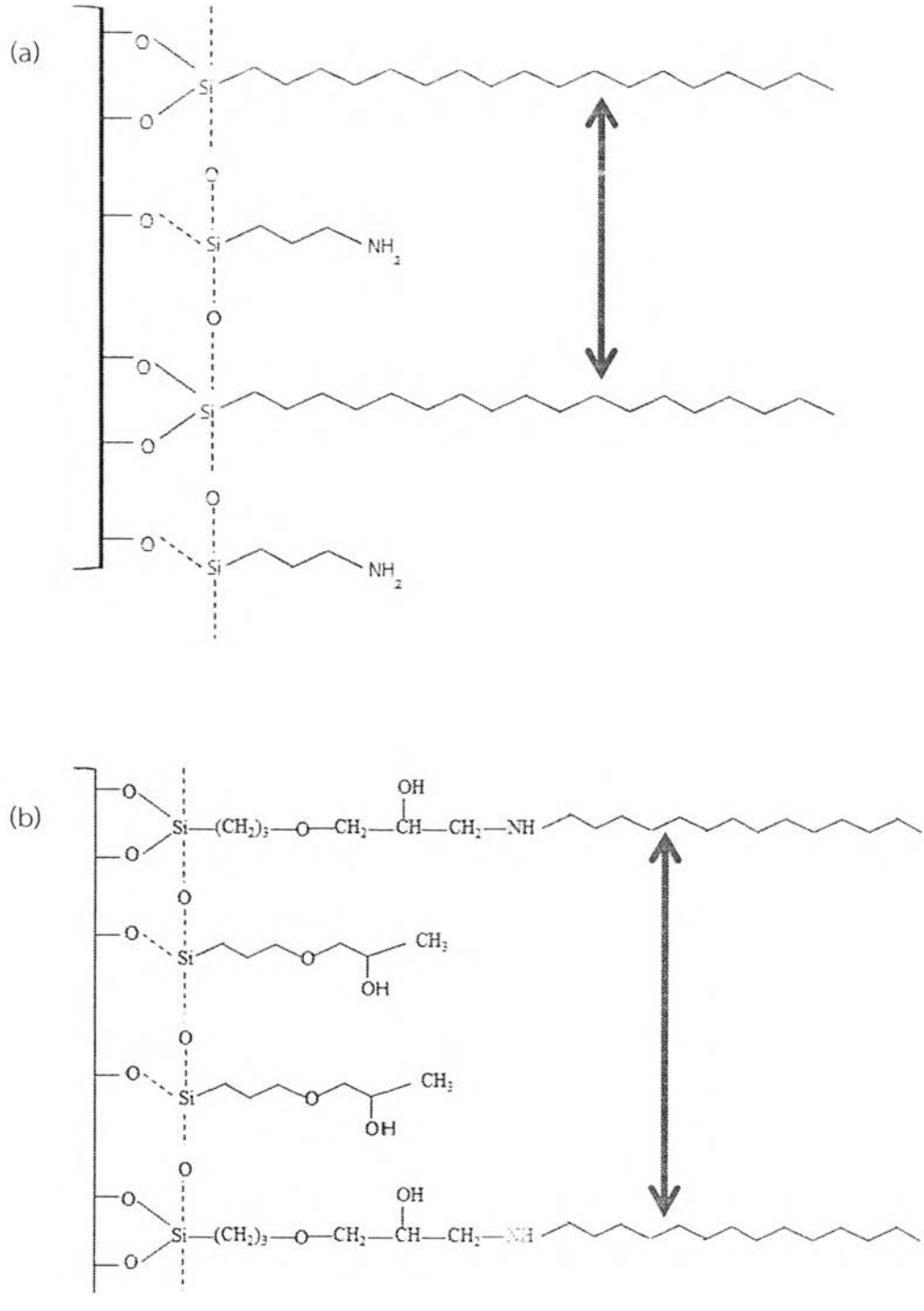

Figure 4.8 The slot of the column (a) C_{18}-AP column (b) C_{14}-amine embedded column.

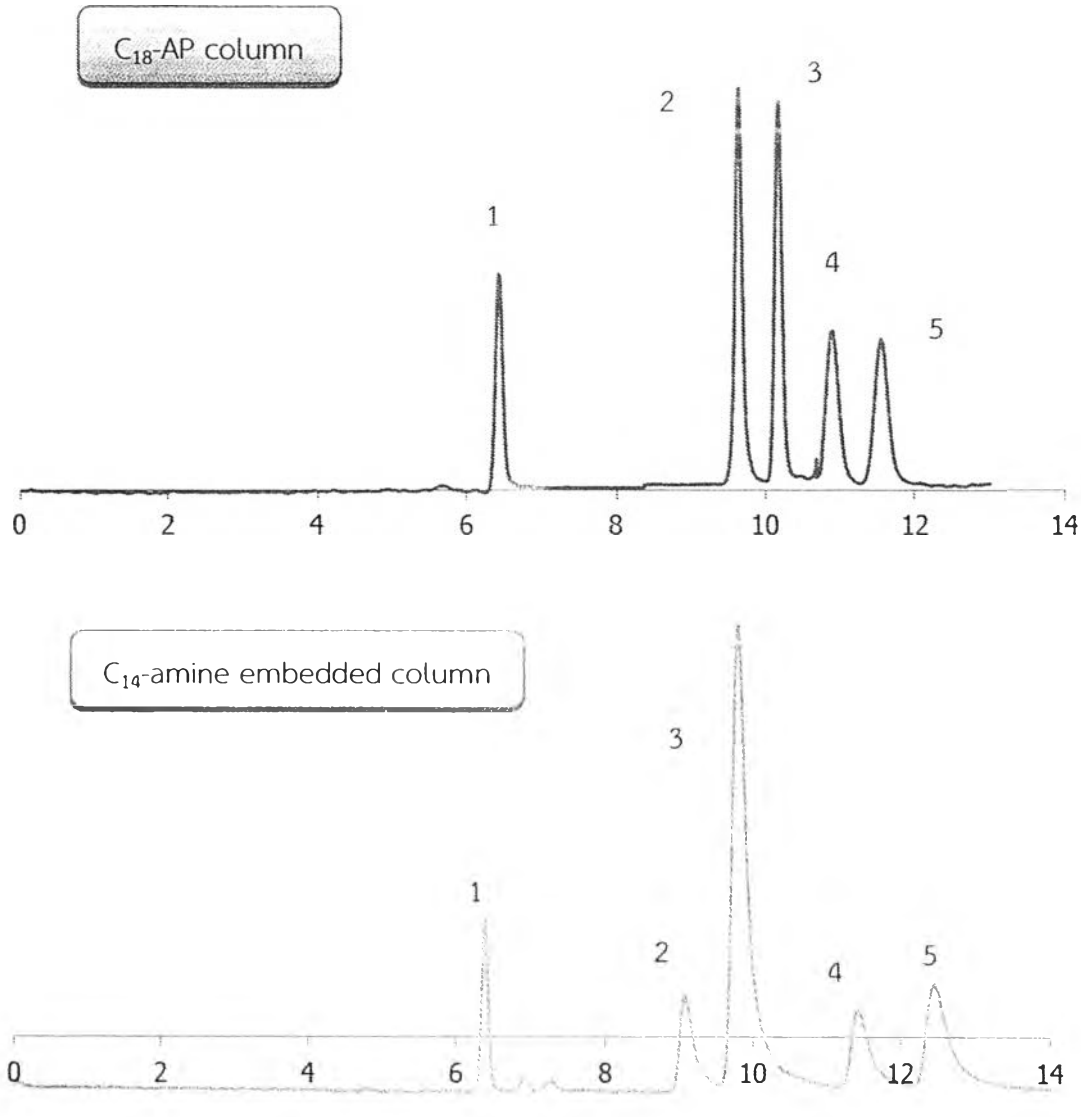

Figure 4.9 Chromatogram for the separation of PAHs using a C_{18}-AP column and a C_{14}-amine embedded column. Mobile phase: 70% methanol, linear velocity: u = 1.0 mm/s, detection wavelength = 210 nm; Compounds: (1) thiourea (2) anthracene (3) fluoranthene (4) triphenylene (5) benzo(k)fluoranthene